Journal of Sound and Vibration (2002) **258**(5), 793–813
doi:10.1006/jsvi.2002.5150, available online at http://www.idealibrary.com on IDEAL®

NUMERICAL MODELLING OF THE SOUND FIELDS IN URBAN STREETS WITH DIFFUSELY REFLECTING BOUNDARIES

J. KANG

*School of Architecture, University of Sheffield, The Arts Tower, Western Bank, Sheffield S*10 2*TN, England*
E-mail: j.kang@sheffield.ac.uk

(*Received* 1 *November* 1999, *and in final form* 5 *February* 2002)

A radiosity-based theoretical/computer model has been developed to study the fundamental characteristics of the sound fields in urban streets resulting from diffusely reflecting boundaries, and to investigate the effectiveness of architectural changes and urban design options on noise reduction. Comparison between the theoretical prediction and the measurement in a scale model of an urban street shows very good agreement. Computations using the model in hypothetical rectangular streets demonstrate that though the boundaries are diffusely reflective, the sound attenuation along the length is significant, typically at 20–30 dB/100 m. The sound distribution in a cross-section is generally even unless the cross-section is very close to the source. In terms of the effectiveness of architectural changes and urban design options, it has been shown that over 2–4 dB extra attenuation can be obtained either by increasing boundary absorption evenly or by adding absorbent patches on the façades or the ground. Reducing building height has a similar effect. A gap between buildings can provide about 2–3 dB extra sound attenuation, especially in the vicinity of the gap. The effectiveness of air absorption on increasing sound attenuation along the length could be 3–9 dB at high frequencies. If a treatment is effective with a single source, it is also effective with multiple sources. In addition, it has been demonstrated that if the façades in a street are diffusely reflective, the sound field of the street does not change significantly whether the ground is diffusely or geometrically reflective.

1. INTRODUCTION

Many investigations have been carried out regarding sound propagation in urban streets [1–14]. A common manner of solving the problem is to use the image source method or ray-tracing techniques. Previous work in this aspect has contributed significantly towards a fundamental understanding of the behaviour of sound in urban streets. However, if there are irregularities on building or ground surfaces, it is necessary to take diffuse reflection into account [2]. Bullen and Fricke, in order to consider the effects of scattering from objects and protrusions in streets, analyzed the sound field in terms of its propagating modes [4]. In a model suggested by Davies, the sound field was assumed to be the sum of a multiply geometrically reflected field and a diffuse field that was fed from scattering at boundaries at each reflection of the geometrical field [5]. Wu and Kittinger, by describing a boundary with a smoothness parameter, developed a simple algorithm for traffic noise prediction [8]. Heutschi suggested modelling sound propagation by a continuous energy exchange within a network of predefined points located on individual plane surfaces, and

0022-460X/02/$35.00

in this way it was possible to define any characteristic directivity pattern for the reflections [9]. Picaut *et al.*, by assuming that the surface irregularities of building façades were adequate to produce diffusion in streets, developed a diffuse sound field model using the mathematical theory of diffusion to predict the sound propagation and reverberation in rectangular streets [11]. Kang carried out a systematic comparison between the sound fields in urban streets resulting from diffusely and geometrically reflecting boundaries, and considerable differences were demonstrated [13].

The objective of this paper is to analyze the fundamental characteristics of the sound fields in urban streets resulting from diffusely reflecting boundaries, and to study the effectiveness of architectural changes and urban design options on noise reduction. This would be useful from the viewpoint of urban street design and street boundary reconditioning. To simulate the sound propagation in urban streets with diffusely reflecting boundaries, a theoretical/computer model has been developed using the radiosity method, an advanced technique for considering diffuse boundaries. This paper begins with a brief description of the model; it then presents some results of numerical modelling.

2. NUMERICAL MODEL

The radiosity method was originally developed for the study of radiant heat transfer in simple configurations [15, 16]. By considering relatively high frequencies and taking the time factor into account, the method has been used in the field of room acoustics [17–19]. With similar principles, the radiosity method can also be used for the study of urban streets. The basic principle of the modelling process is to divide the boundaries of a street into a number of patches, and then to simulate the sound propagation in the street by energy exchange between the patches [13].

A computer model, RASCL, has been developed to consider a rectangular urban street with a length of X, width of Y and height of Z, as illustrated in Figure 1. For convenience, the ground is called G, and the two façades are defined as A and B respectively. A sound source S is positioned at (S_x, S_y, S_z). In RASCL it is assumed that the façades are diffusely reflective, namely, the sound energy reflected from a patch is dispersed over all directions according to the Lambert cosine law. The ground can be either diffusely or geometrically

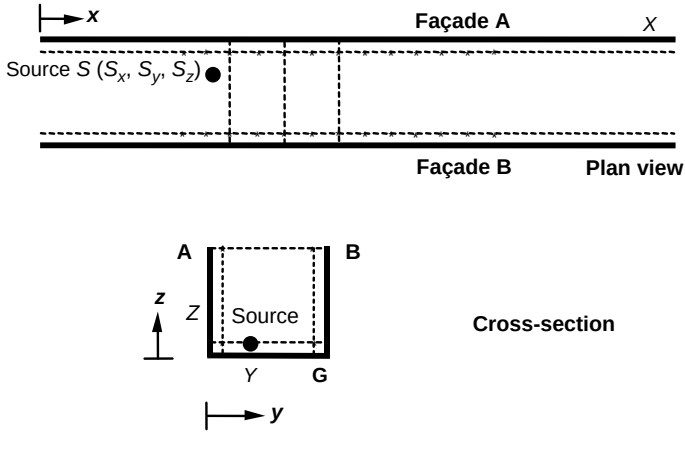

Figure 1. Plan and cross-section of an idealized rectangular street. – – –, receiver planes for the calculations in Figures 6–10; *, receivers for the calculations in Figures 11–16 and Table 1.

reflective. In sections 2.1–2.3 all the street boundaries are assumed as diffusely reflective. In section 2.4 the situation with geometrically reflecting ground is considered.

2.1. PATCH DIVISION AND FORM FACTOR

First consider the situation where the façades and ground are all diffusely reflective. Each of the three boundaries is divided into a certain number of rectangular patches. The energy moving between pairs of patches depends on a form factor, which is defined as the fraction of the sound energy diffusely emitted from one patch which arrives at the other by direct energy transport.

Clearly, the simulation is more accurate with finer patch parameterization, but there is a square-law increase of calculation time in the number of patches. To optimize the calculation, in RASCL the boundaries are so divided that a patch is smaller when it is closer to an edge. This is because, for a given patch size, numerical determination of form factors becomes less accurate as the patch moves closer to an edge [20]. For the convenience of computation, the division of boundaries is in the manner of a geometrical series. If a boundary dimension is not large (such as along the width) and the patch number is not great, the patch size increases from the edges to the centre. For a relatively large dimension and/or patch number, to avoid extreme differences between patches, the patch size varies only in a certain range from the edges, and becomes constant in the remaining of the boundary.

A key stage of the modelling process is the determination of form factors. In a rectangular urban street, the relative location between any two patches is either orthogonal or parallel. For orthogonal patches, in RASCL the form factor is calculated by using Nusselt's method [19, 21]. Computing a form factor by this method is equivalent to projecting the receiving patch onto a unit hemisphere centred about the radiation patch, then projecting this projected area orthographically down onto the hemisphere's unit circle base, and finally dividing by the area of the circle. For parallel patches, the form factor is calculated by a method developed by Cohen and Greenberg [22], which involves projecting the receiving patch onto the upper half of a cube centred about the radiation patch.

2.2. ENERGY EXCHANGE

The starting point of the energy exchange process is to distribute the source energy to the patches. Assume that the sound source $S(S_x, S_y, S_z)$ generates an impulse at time $t = 0$. The basic principle for distributing the source energy to patches is that the energy fraction at each patch is the same as the ratio of the solid angle subtended by the patch at the source to the total solid angle. The source directionality can be considered using a weighting factor in the direction of each patch.

The patches can now be regarded as sound sources, which are called first order patch sources below. The radiation strength of a first order patch source depends on the energy at the patch received from source S as well as the patch absorption. In RASCL, for convenience, an angle-independent absorption coefficient is considered for each patch.

In addition, air absorption when sound transfers from source S to patches and from one patch to another should be taken into account. In RASCL, this is expressed by an intensity-related attenuation constant M (Np/m). The absorption by vegetation, $V_{,}$ is similarly considered.

By the form factors obtained above (see section 2.1), the sound energy of each first order patch source can be re-distributed to other patches and consequently, the second order

patch sources can be generated. By continuing this process of energy exchange the kth order patch sources can be obtained ($k = 1, \ldots, \infty$). It is important to note that the above process is 'memory-less', that is, the energy exchange between patches depends only on the form factors and the patch sources of preceding order. By considering this feature, the requirement for computer storage can be significantly reduced.

A patch source is expressed in a form of energy response. For the configuration in Figure 1, a kth order patch source on a street boundary is calculated by summing the contribution from all the $(k-1)$th order patch sources on the other two boundaries. For example, to calculate the sound energy of a kth order patch source on the ground at time t, $G_k(t)_{l,m}$, the contribution from the patches on the two façades should be summed:

$$G_k(t)_{l,m} = \sum_{l'=1}^{N_X}\sum_{n'=1}^{N_Z} AG_{(l',n'),(l,m)} A_{k-1}\left[t - \frac{d_{AG(l',n'),(l,m)}}{c}\right]_{l'n'} + \sum_{l'=1}^{N_X}\sum_{n'=1}^{N_Z} BG_{(l',n'),(l,m)} B_{k-1}\left[t - \frac{d_{BG(l',n'),(l,m)}}{c}\right]_{l'n'} \quad (1)$$

where $l, l' = 1, \ldots, N_X$, $m, m' = 1, \ldots, N_Y$ and $n, n' = 1, \ldots, N_Z$ are the patches along the length, width and height, respectively. $AG_{(l',n'),(l,m)}$ is the form factor from radiation patch $A_{l',n'}$ to receiving patch $G_{l,m}$, with the consideration of patch absorption as well as the absorption from air and vegetation. $A_{k-1}[t - d_{AG(l',n'),(l,m)}/c]_{l',n'}$ is the energy of the $(k-1)$th order patch source $A_{l',n'}$ at time $t - d_{AG(l',n'),(l,m)}/c$. $d_{AG(l',n'),(l,m)}$ is the mean beam length between patches $A_{l',n'}$ and $G_{l,m}$. $BG_{(l',n'),(l,m)}$, $B_{k-1}[t - d_{BG(l',n'),(l,m)}/c]_{l',n'}$ and $d_{BG(l',n'),(l,m)}$ are defined accordingly. With a similar manner to equation (1), the sound energy of a kth order patch source on the façades can be determined.

In RASCL the mean beam length between two patches is determined by subdividing each patch into u by v ($u, v \geqslant 1$) elements and then calculating the average distance between each pair of elements. A similar method is also used for calculating the distance from a patch to source S or to a receiver. When patches are reasonably small, it is often sufficiently accurate to use $u = v = 1$, namely the distance to the patch centre.

2.3. RECEIVER

Now consider the energy response at a receiver R (R_x, R_y, R_z). For each order of energy exchange between patches, the sound energy at the receiver contributed from each patch source should be considered. For example, at time t the energy contribution from all the kth order patch sources on the ground can be determined by

$$E_k(t)_G = \sum_{l=1}^{N_X}\sum_{m=1}^{N_Y}\left[\frac{G_k(t - R_{l,m}/c)_{l,m}}{\pi R_{l,m}^2}\cos(\xi_{l,m})\right]e^{-(M+V)R_{l,m}}, \quad (2)$$

where $\xi_{l,m}$ is the angle between the normal of patch $G_{l,m}$ and the line joining receiver R and patch $G_{l,m}$, $R_{l,m}$ is the mean beam length between receiver R and patch $G_{l,m}$, and $e^{-(M+V)R_{l,m}}$ represents the absorption of air and vegetation.

By considering the energy from all orders of patch sources as well as the direct energy transport from source S, the energy response at receiver R can be given by

$$L(t) = 10\lg\{E_d(t) + \sum_{k=1}^{\infty}[E_k(t)_G + E_k(t)_A + E_k(t)_B]\} - L_{ref}, \quad (3)$$

where $E_k(t)_A$ and $E_k(t)_B$ are the energy contribution from the patches on façades A and B, $E_d(t)$ represents the direct sound and L_{ref} is the reference level.

With the energy response the steady state sound pressure level (SPL) at receiver R can easily be calculated. The decay curve can be obtained by the reverse-time integration of $L(t)$. Consequently, reverberation time, which has been demonstrated to be a useful index for streets [23, 24], can be determined. In RASCL both the early decay time (EDT) and RT30 are considered. The EDT is obtained from the initial 10 dB of the decay. RT30 is determined using the rate of decay given by the linear regression of the measured decay curve from a level 5 dB below the initial level to 35 dB below.

After each order of energy exchange, the total residual energy on all patches is calculated. Calculation stops when the total energy reduces to a certain amount, typically 10^{-6} of the energy of source S.

2.4. GEOMETRCALY REFLECTING GROUND

In sections 2.1–2.3 it is assumed that the ground is diffusely reflective, but RASCL can also consider geometrically reflecting ground. A geometrically reflecting ground can be treated as a mirror and the sound source S and the patch sources will have their images, as illustrated in Figure 2. The initial energy in the patch sources on the façades is from the sound source S as well as its image, S'. For the latter, the absorption coefficient of the ground is taken into account. During the energy exchange process, the energy in a patch source on a façade, say A, is calculated by summing the contribution from all the patch sources on façade B and its image, B′. At receiver R, for each order of energy exchange between patches, the sound energy contributed from each patch source and their images is summed. In addition to the multiple reflections considered above, the direct sound and the first reflection from source to receiver through the ground are also included.

2.5. MODEL VALIDATION

To validate the model, a comparison has been made between the prediction by RASCL and the measurements carried out by Picaut *et al.* [11] in a 1 : 50 scale model of an urban

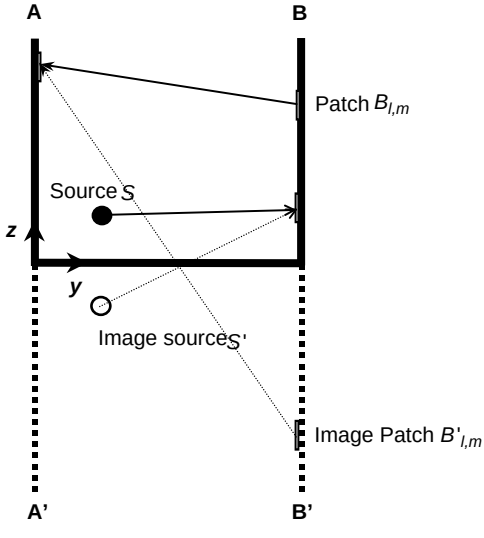

Figure 2. Cross-section of an idealized rectangular street with diffusely reflecting façades and geometrically reflecting ground, showing the distribution of source energy and energy exchange between patches.

street. The street length, width and height are 96, 8 and 12 m respectively. The model façades follow a statistic distribution extracted from an actual Haussmann building façade [14]. This type of façades is rather common in European cities and they are considered as diffusely reflective. The measurement data given by Picaut *et al.* [11] are based on the average in the frequency range 400 Hz to 1·6 kHz, so that the calculation is also in this range. The measured absorption coefficient of the façades is about 0·05 at middle frequencies. The ground is acoustically smooth and highly reflective, so that an absorption coefficient of 0·01 is used in the calculation. A point source is used in the calculation, which corresponds to the spark source used in the measurement. The source is positioned at (16, 4, 2)m, and the receivers are along line (20–95, 4, 2)m with an interval of 2·5 m.

A comparison of sound distribution between calculation and measurement is shown in Figure 3, where the *SPL*s are normalized with respect to the value at $x = 20$ m. In the calculation, the sound power level of the source is set as 0 dB. It can be seen that the agreement is very good, generally within $\pm 1{\cdot}5$ dB accuracy. In Figure 3 is also shown the calculated, *SPL* distribution based on diffusely reflecting ground. It is seen that the result is rather close to that with geometrically reflecting ground. The *SPL* difference between the two kinds of ground increases with increasing source–receiver distance. At 79 m from the source, the *SPL* with diffusely reflecting ground is about 3 dB lower than that with geometrically reflecting ground. An important reason is that with more diffusely reflecting boundaries, the sound path length generally becomes longer [13]. For comparison, the calculation based on the image source method, namely, by assuming that all the street boundaries are geometrically reflective, is also shown in Figure 3. It is seen that the result is significantly different from the measured values. At 79 m from the source, the *SPL* difference is about 10 dB.

In Figure 4 is shown the comparison in reverberation time between calculation and measurement. The agreement is very good, with an average difference of 6%. The reverberation time based on the image source method is also shown in Figure 4. It is seen that the calculated values are much longer than the measured data, at about 180%. A

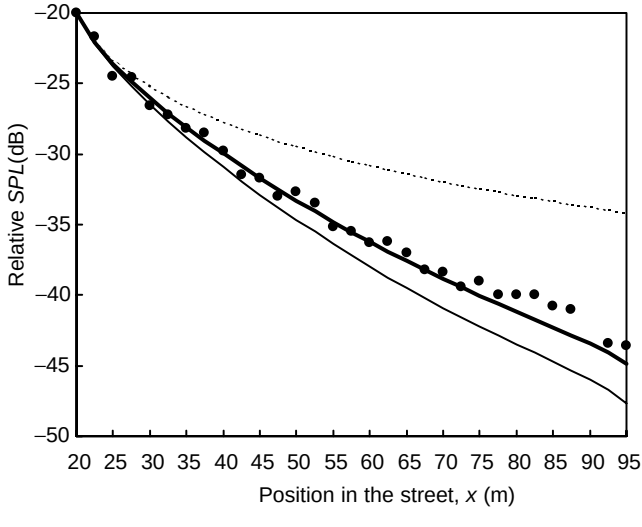

Figure 3. Comparison of *SPL* attenuation along the length between measurement [11] (●) and calculation (▬, RASCL with geometrically reflecting ground; ▬, RASCL with diffusely reflecting ground; ····, image source method).

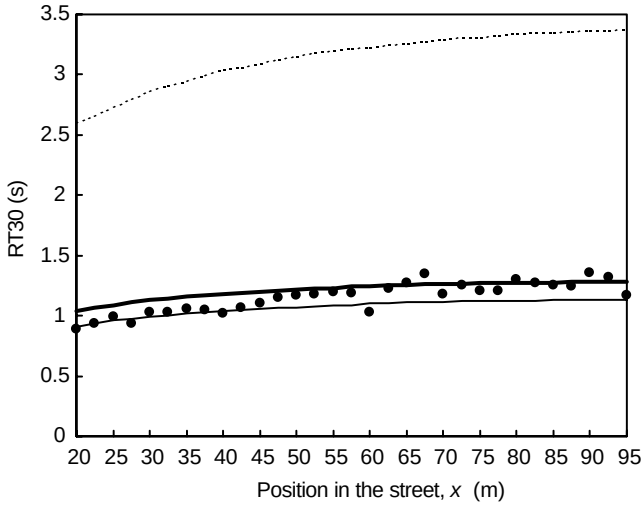

Figure 4. Comparison of RT30 between measurement [11] (●) and calculation (▬, RASCL with geometrically reflecting ground; —, RASCL with diffusely reflecting ground; · · · · · ·, image source method).

main reason is that in comparison with the sound decay resulting from geometrically reflecting boundaries, if the façades become diffusely reflective, the initial energy is increased slightly [25] and the later energy due to flutter echo type of reflections is decreased substantially. This can be clearly seen by comparing typical decay curves in the two cases, as shown in Figure 5, where the receiver is at (75, 4, 2) m, namely, the source–receiver distance is 59 m. The calculated reverberation time and decay curve, by assuming the ground as diffusely reflective, are also shown in Figures 4 and 5. It is seen that the result is rather close to that with geometrically reflecting ground.

In the calculation using RASCL there is an initial stage of determining patch division, including patch numbers and ratios between adjacent patches, so that a required accuracy in calculating form factors and the source energy distribution can be achieved. The accuracy in calculating form factors can be evaluated by the fact that the sum of the form factors from any patch to all the other patches should be unity. The accuracy in distributing the source energy to patch sources can be similarly evaluated. For the above street, the patch numbers used are $X = 16$ and $Y = Z = 12$. Along the length, the patch size increases from $l = 1$ to 15, decreases from $l = 46$ to 60, and is constant between $l = 16$ and 45. For the varied patch sizes, the ratio between two adjacent patches is $q_x = 1{\cdot}05$. Along the width and height, the patch size increases from the edges to the centre with a ratio of $q_y = q_z = 1{\cdot}1$. Using these parameters RASCL calculates the form factors and the source energy distribution on patches accurate to three decimal places.

Overall, through the above comparison and analysis the accuracy and effectiveness of RASCL is demonstrated. It is also shown that if the façades in a street are diffusely reflective, there is no significant difference in the sound field of the street whether the ground is diffusely or geometrically reflective.

By considering more boundaries, the above algorithms can be used for rectangular enclosures. Such a model was shown to correctly calculate the acoustic characteristics of a cube [19]. This can be regarded as a further validation of the algorithms. Moreover, comparisons were made between the calculated reverberation times by the program and the measured values in the scale models of a regularly shaped enclosure and a flat enclosure, and the agreement was very good [19]. Furthermore, a series of tests was made

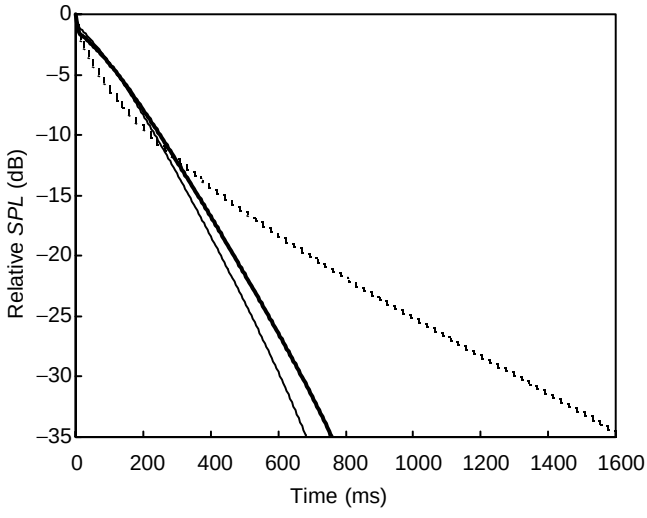

Figure 5. Comparison of the decay curves obtained using three calculation methods: ▬, RASCL with geometrically reflecting ground; ▬, RASCL with diffusely reflecting ground; · · · · · ·, image source method. The receiver is at (75, 4, 2) m, namely, the source–receiver distance is 59 m.

in regularly shaped enclosures with unevenly distributed boundary absorption, and there was good agreement between the calculation by the program and the result obtained using the classic theory [26].

2.6. DISCUSSION

As indicated previously, RASCL is applicable for diffusely reflecting street boundaries. However, if most street boundaries are largely diffusely reflective in a street, due to the effect of multiple reflections, the sound field should still be close to that resulting from purely diffusely reflecting boundaries [27]. This is supported by the result that if the façades in a street are diffusely reflective, there is no significant difference between the sound fields resulting from geometrically and diffusely reflecting ground. Moreover, although the street grounds are usually geometrically reflective, vehicles, pedestrians, and street furniture (e.g., bushes, lampposts, fences, barriers, benches, telephone boxes and bus shelters) may bring considerable diffuse reflection. Furthermore, there seems to be strong evidence that even untreated boundaries produce diffuse reflections [28]. This may further extend the application range of the model.

It is noted that RASCL is an energy-based model, which ignores wave effects and thus the application range is mainly at middle and high frequencies. Given that with diffusely reflecting boundaries the interference patterns may not be significant in a street, especially for broadband sound sources and relatively high frequencies, in RASCL the ground effect [29–32] is not considered [2]. Temperature- or wind-gradient-induced refraction is also not taken into account. At lower frequencies, street boundaries may tend to be more geometrically reflective and thus, it would be important to consider wave effects. For a single street with geometrically reflecting boundaries, Iu and Li developed a coherent model using the image source method, and it was demonstrated that such a model can give a better prediction than incoherent model at low frequencies [12, 33].

3. COMPUTATION

Using RASCL a series of calculations has been carried out in a number of hypothetical rectangular streets. The street geometry represents certain types of urban street in Europe [34, 35]. Firstly, a typical street configuration is considered in order to investigate the characteristics of the sound fields in urban streets resulting from diffusely reflecting boundaries. Then the effectiveness of architectural changes and urban design options on noise reduction, especially on increasing sound attenuation along the length, is studied. For the sake of convenience, it is assumed that all the boundaries are diffusely reflective. Note that the source–receiver distance below refers to the horizontal distance along the street length.

3.1. A TYPICAL URBAN STREET

The street configuration corresponds to Figure 1. The street length, width and height are 120, 20 and 18 m respectively. The buildings are continuous along the street and of constant height on both sides. A point source is positioned at (30, 6, 1) m. The façades and ground are assumed to have a uniform absorption coefficient of 0·1 [3, 14]. The patch divisions are similar to those used in the calculation described in section 2.5. For the sake of convenience, absorption from air and vegetation is not considered.

The *SPL* distribution on a horizontal plane of 1 m above the ground is shown in Figure 6(a), where the sound power level of the source is set as 0 dB. It is noteworthy that although the boundaries are diffusely reflective, the *SPL* varies significantly on the plane. Along $y = 10$ m, for example, the *SPL* attenuation is 22·7 dB at source–receiver distances of 5–90 m (i.e., 26·7 dB/100 m). As expected, the *SPL* variation becomes less when the horizontal plane is farther from the source. In Figure 6(b) the sound distribution on a plane of 18 m above the ground is shown. Along $y = 10$ m the *SPL* attenuation at source–receiver distances of 5 m through to 90 m is 16·8 dB (i.e., 19·8 dB/100 m). By comparing Figures 6(a) and (b), it can be seen that the *SPL* difference between the two planes decreases with increasing distance from the source. Beyond the source–receiver distance of 10–15 m, this difference is less than 1–2 dB, which means that in this range the sound distribution in cross-section is rather even. This can also be seen in Figure 7, where the sound distributions along six lines, (1–120, 1, 1) m, (1–120, 5, 1) m, (1–120, 19, 1) m, (1–120, 1, 18) m, (1–120, 5, 18) m, and (1–120, 19, 18) m, are compared.

The sound distribution on a vertical plane at a distance of 1 m from façade A is shown in Figure 8(a). At $x = 30$ m, namely the source position, the *SPL* variation with height is significant, at about 8 dB. With increasing distance from the source in the length direction, the *SPL* variation with height decreases rapidly. Beyond $x = 50$ m, it becomes less than 1 dB. In Figure 8(b) the sound distribution on a vertical plane which is 1 m from façade B is shown. It can be seen that, because façade B is farther from the source than façade A, the *SPL* variation with height is generally less than that in Figure 8(a). At $x = 30$ m, for example, the variation is only 2·5 dB.

The sound distribution in three typical cross-sections at $x = 35$, 45 and 55 m is shown in Figure 9. It can be seen that in the cross-section of $x = 35$ m the *SPL* variation is 7·5 dB, and with increasing source-receiver distance this variation decreases rapidly. Beyond $x = 55$ m, the variation is usually less than 1·5 dB.

Generally speaking, the *SPL* attenuation curve along the length is concave. In other words, the attenuation per unit distance becomes less with the increase of source-receiver distance.

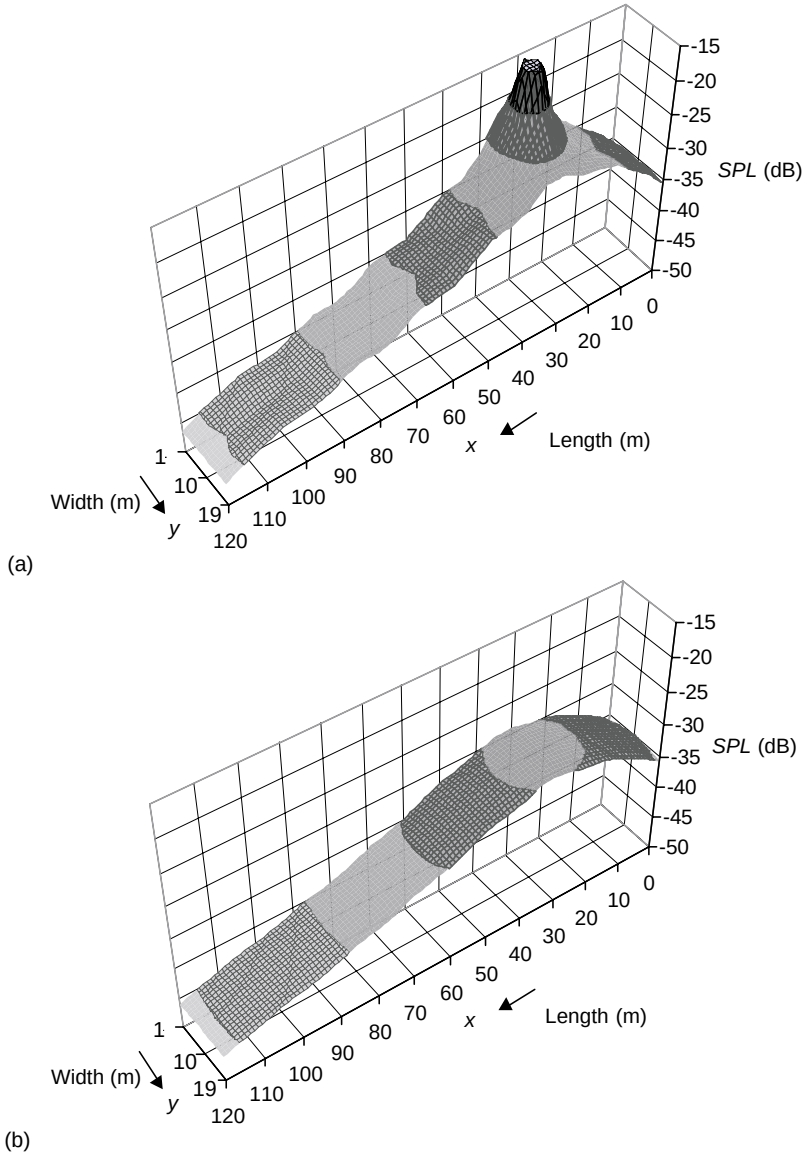

Figure 6. *SPL* distribution on two horizontal planes in a typical street: (a) 1 m above the ground; (b) 18 m above the ground.

3.2. STREET ASPECT RATIO

To investigate the effect of street aspect ratio on the sound field, a range of street heights from 6 m to 54 m is considered, which corresponds to the height/width ratio of 0·3 to 2·7. Other configurations are the same as those in Figures 1 and 6–9. Calculations show that the *SPL* attenuation along the length becomes less with increasing street height. An apparent reason is that with a greater street height, less energy can be reflected out of the street canyon. In Figure 10 is shown the difference between $Z = 6$ and 54 m in *SPL* on a horizontal plane at a distance of 1 m from the ground. In the near field, say within 10 m

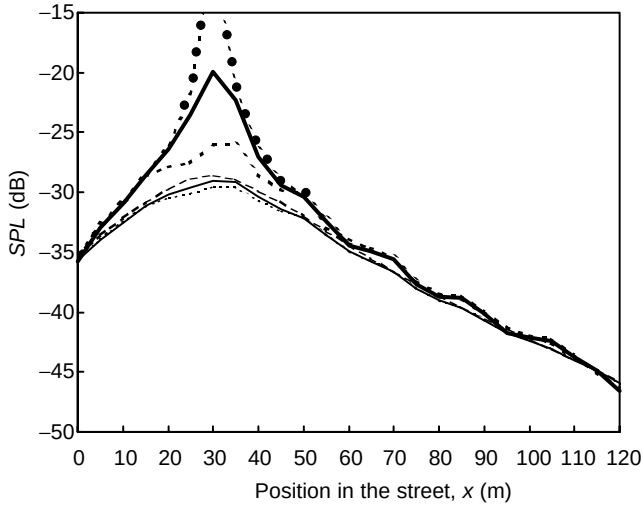

Figure 7. *SPL* distribution along a typical street: ▬, (0–120, 1, 1) m; – ● –, (0–120, 5, 1) m; ▪▪▪, (0–120, 19, 1) m; ——, (0–120, 1, 18) m; – – –, (0–120, 5, 18) m; · · · · · ·, (0–120, 19, 18) m.

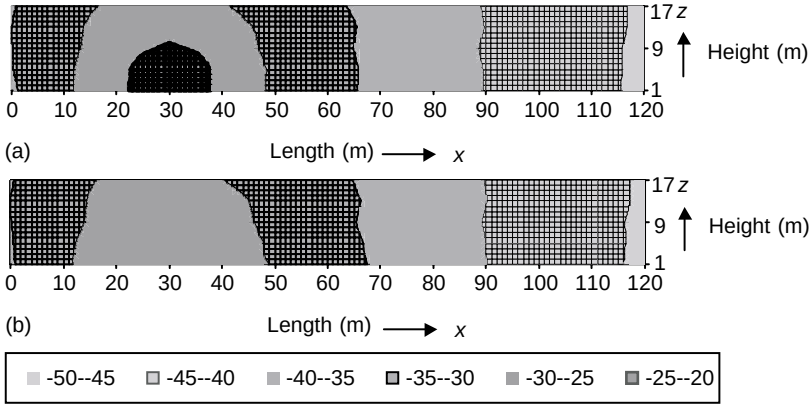

Figure 8. *SPL* (dB) distribution on two vertical planes in a typical street: (a) 1 m from façade A; (b) 1 m from façade B.

from the source, the difference between the two street heights is insignificant, which indicates the strong influence of the direct sound. With the increase of source–receiver distance, the effect of boundary reflections becomes more important and thus, the difference between the two street heights becomes greater. Beyond about $x = 110$ m, there is a decrease in the *SPL* difference. This is because there is no boundary beyond $x = 120$ m and consequently, the effect of boundary reflections is diminished.

It is noteworthy that with $Z = 54$ m, although the street height/width ratio is rather great, the *SPL* still varies significantly along the length. Along $y = 10$ m, for example, the *SPL* attenuation at source-receiver distances of 5–90 m is 19·3 dB (i.e., 22·7 dB/100 m).

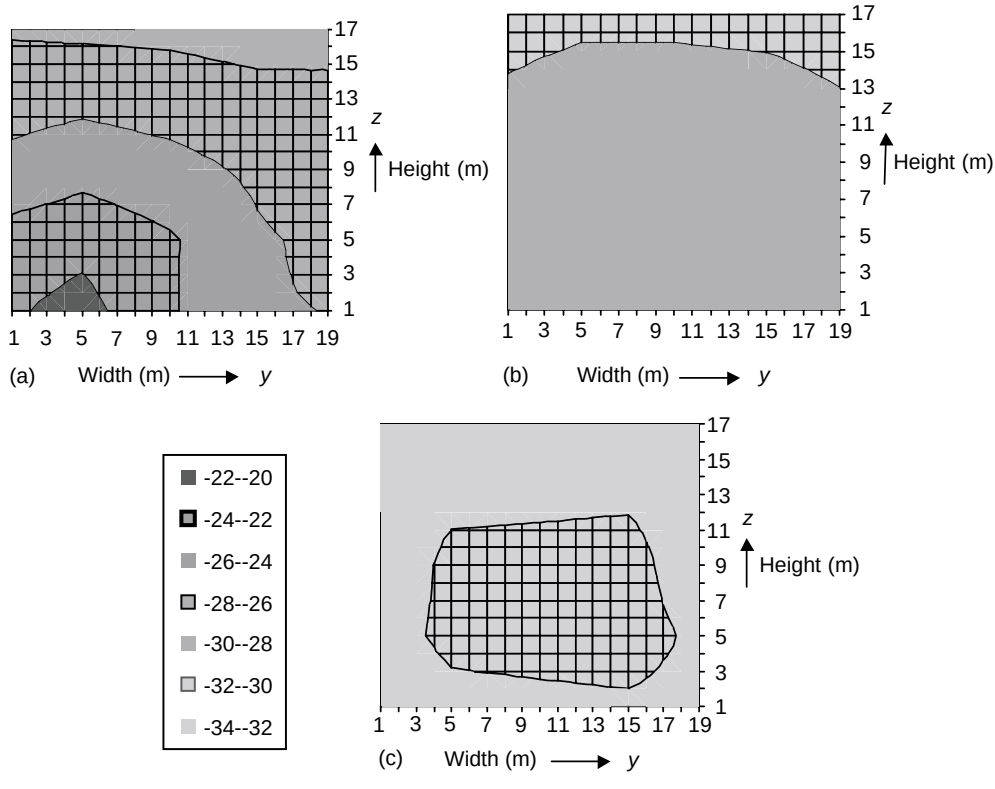

Figure 9. *SPL* (dB) distribution in three cross-sections in a typical street: (a) 5 m from the source; (b) 15 m from the source; (c) 25 m from the source.

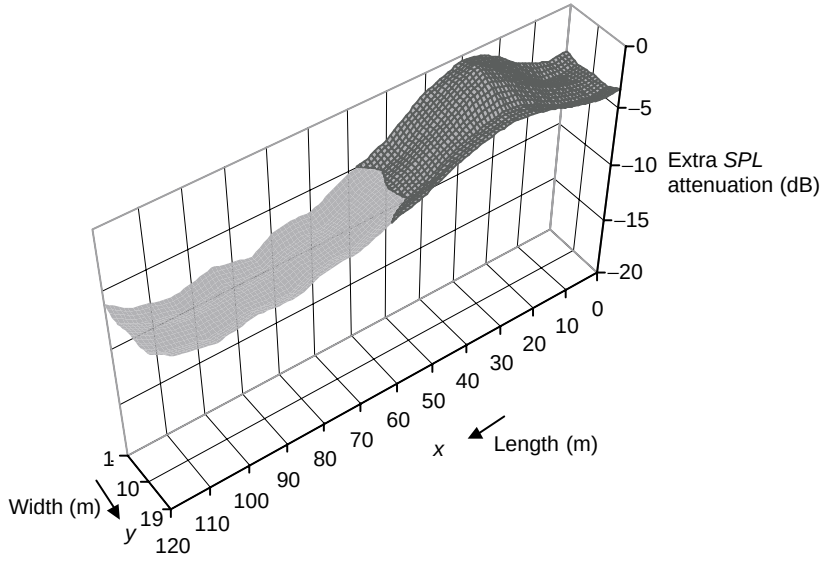

Figure 10. Extra *SPL* attenuation on a horizontal plane at a distance of 1 m above the ground caused by reducing street height from 54 to 6 m.

3.3. BOUNDARY ABSORPTION AND BUILDING ARRANGEMENTS

In a previous study [13], it has been demonstrated that by replacing geometrically reflecting boundaries in a street with diffusely reflecting boundaries, considerable extra attenuation can be obtained. This section analyzes the effectiveness of boundary absorption and building arrangements upon the sound attenuation along the length in the case of diffusely reflecting boundaries. For the sake of convenience, the configurations of the boundary treatments correspond to the patch division. The effectiveness of a treatment is evaluated by the extra *SPL* attenuation caused by the treatment with reference to the typical case described in section 3.1. In each cross-section four typical receivers are considered, which represent relatively high and low *SPL* in the cross-section. Correspondingly, the calculation of sound attenuation along the length is based on the average of four receiver lines, namely (31–90, 2, 1) m, (31–90, 2, 18) m, (31–90, 18, 1) m, and (31–90, 18, 18) m, as illustrated in Figure 1.

The extra attenuation caused by evenly increasing the absorption coefficient of all the three boundaries from 0·1 to 0·3, 0·5, 0·7 and 0·9 is shown Figure 11. It can be seen that with increasing absorption coefficient, the extra attenuation increases proportionally. With an absorption coefficient of 0·9 the extra attenuation is 6–7 dB along the length, which is significant and also approximately indicates the maximum effectiveness of boundary absorption on noise reduction. Recently, there have been considerable works on outdoor sound absorbers [32, 36–37], mainly for noise barriers, but they are also useful for urban streets. Moreover, open windows and gaps between buildings can be regarded as sound energy sinks.

In Figure 11 it is seen that the extra attenuation generally increases with increasing source–receiver distance. This is mainly because in the near field the direct sound plays an important role and thus, the boundary absorption is relatively less significant. It is also seen in Figure 11 that in the far field there is a slight decrease in the extra attenuation, and this is more noticeable with increasing absorption coefficient. The major reason for this is that, with increasing source–receiver distance, the sound attenuation due to distance becomes more important and the role of reflection order, which is highly related to the

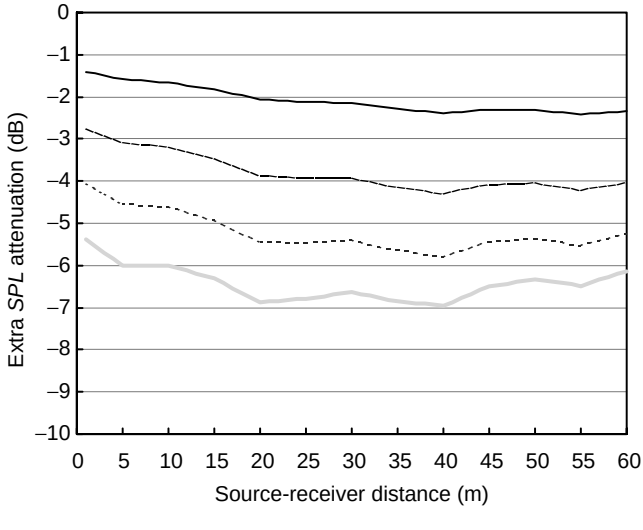

Figure 11. Extra *SPL* attenuation caused by increasing the absorption coefficient of all the three boundaries from $\alpha = 0{\cdot}1$ to 0·3 (——), 0·5 (– – –), 0·7 (· · · · ·) and 0·9 (——).

effectiveness of boundary absorption, becomes relatively less important. The periodicity in Figure 11 and in some other figures in this section is a phenomenon related to the numerical process. The periodicity patterns vary with different patch division.

In Figure 12 is shown the effect of absorbers over the ground. The absorbers are arranged along the length, and four cases are considered: Case I, absorbers from $y = 1{\cdot}23$ to 3·06 m and from $y = 16{\cdot}94$ to 18·77 m; Case II, absorbers from $y = 5{\cdot}85$ to 14·15 m; Case III, absorbers from $y = 0$ to 5·85 m and from $y = 14{\cdot}15$ to 20 m; and Case IV, absorbers over the entire ground. The ratios of absorber to ground area in the four cases are 18·3, 41·5, 58·5 and 100%, respectively. To demonstrate the maximum noise reduction by each treatment, in the calculation the absorption coefficient of the absorbers is assumed as 1. In Figure 12 it can be seen that from Cases I to IV the extra attenuation increases continuously. In Case IV, where the ground is totally absorbent, the extra attenuation is about 3–4 dB. It appears that the extra attenuation is approximately proportional to the absorber area.

The effect of façade absorption is shown in Figure 13. Four cases are considered: Case V, absorbers along the length, façade B only; Case VI, absorbers along the length, façades A and B; Case VII, absorbers along the height, façade B only; and Case VIII, absorbers along the height, façades A and B. For the sake of convenience, the absorber locations correspond to the patch division in the calculation. For each treated façade, the ratio of absorber to façade area is 50%. The absorption coefficient of the absorbers is again assumed as 1. From Figure 13 it can be seen that with absorbers on façade B only, the extra attenuation is about 1–2 dB, and with absorbers on both façades, the extra attenuation is around 2–4 dB. It is interesting to note that with a given absorber area there

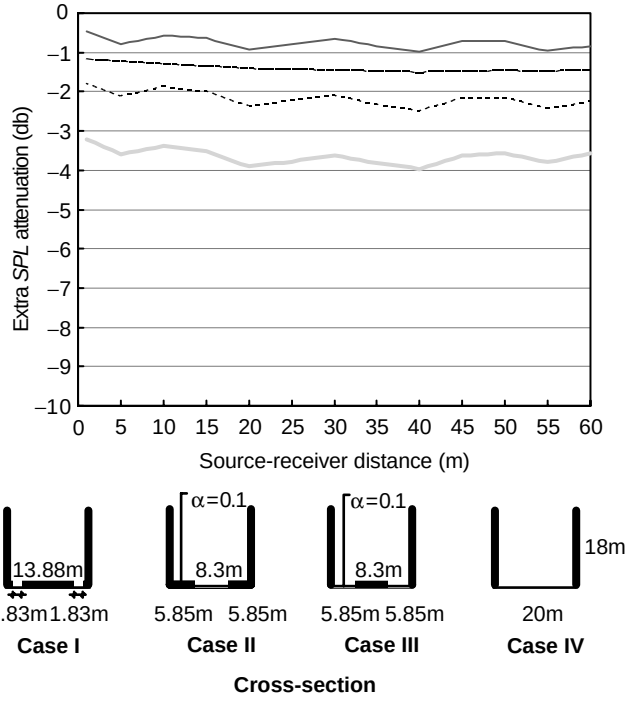

Figure 12. Extra *SPL* attenuation caused by placing absorbers ($\alpha = 1$) on the ground: ——, Case I; – – –, Case II; · · · · · ·, Case III; ——, Case IV.

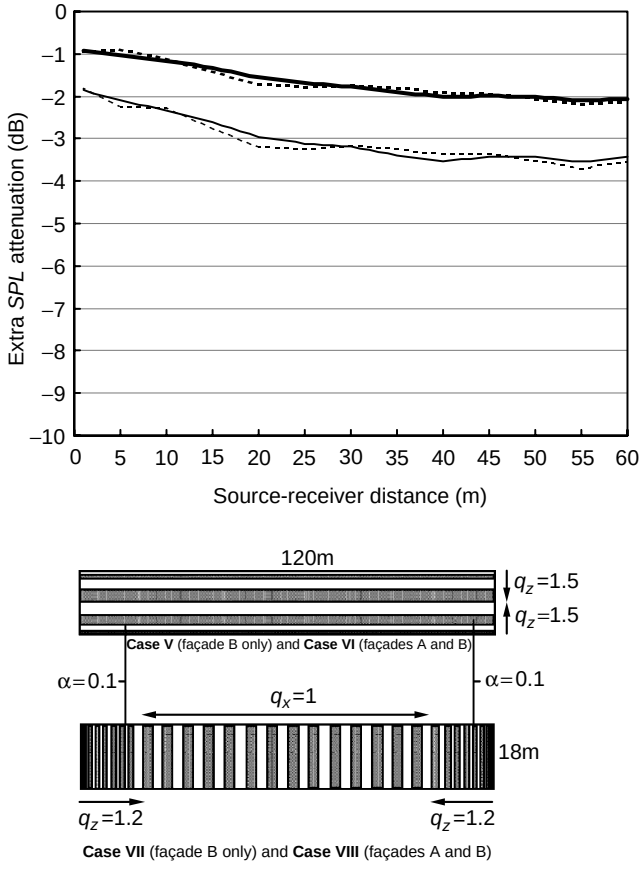

Figure 13. Extra *SPL* attenuation caused by placing absorbers ($\alpha = 1$) on façades: ▬, Case V; ▪▪▪, Case VII, ▬, Case VI; · · · · · ·, Case VIII. The grey areas represent absorbers. q_x and q_z are the ratios between two adjacent patches along the length and height respectively.

is almost no difference in sound attenuation between vertically and horizontally distributed absorption. This suggests that with diffusely reflecting boundaries, the arrangement method of absorbers on a boundary plays an insignificant role for the sound field.

The extra sound attenuation caused by reducing the height of façade B to 15·25 m (Case IX), 9 m (Case X), 2·75 m (Case XI) and 0 m (Case XII) is shown in Figure 14. As expected, from Cases IX to XII the extra attenuation increases continuously. With Case XII, the influence of façade B upon sound attenuation along the street can be clearly seen, which is about 2–4 dB.

For a given amount of absorption, it is useful to investigate the effect of strategic arrangement of the absorbers in cross-section. Cases IV, VI and XII have approximately the same amount of absorption but different absorber locations. By comparing Figures 12–14, it can be seen that the extra sound attenuation is similar in Cases VI and XII, but is systematically greater in Case IV, particularly in the near field. A major reason is that, due to the low source height, the sound energy distributed to the first order sources on the ground is considerably more than that on the façades, especially in the near field.

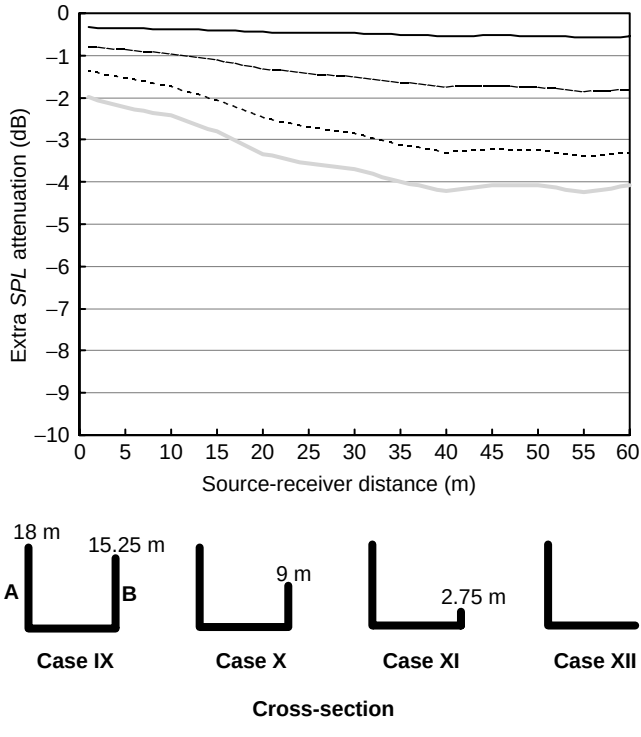

Figure 14. Extra *SPL* attenuation caused by reducing the height of façade B: ——, Case IX; – – –, Case X; · · · · · ·, Case XI; ——, Case XII.

Consequently, absorbers are more effective when they are on the ground than on façades. With increasing source–receiver distance, however, multiple reflections become dominant and the energy distribution on the first order sources is relatively less important. As a result, in the far field, the extra attenuation in Cases IV, VI and XII is almost the same. Further calculation regarding absorption distribution shows that the sound attenuation along the length is the highest if certain absorbers are arranged on one boundary and the lowest if they are evenly distributed on all boundaries.

It is also interesting to investigate the effect of gaps between buildings. In Figure 15 is shown the extra sound attenuation in two cases, namely, Case XIII, one gap on façade B from $x = 48$ to 72 m; and Case XIV, one gap on façade A and one gap on façade B, both from $x = 48$ to 72 m. In the calculation, the absorption coefficient of the gap is assumed to be 1. The main reason for this assumption is that for an urban element consisting of a major street and two side streets, it has been demonstrated that if a source is in the major street and all the boundaries are diffusely reflective, the reflected energy from the side streets to the major street is negligible [38, 39]. It is noted that the leakage of sound through the gaps is a frequency-dependent process and the situation becomes more complicated if low frequencies are considered. From Figure 15 it can be seen that in the length range containing the gap(s), there is a considerable extra *SPL* attenuation, which is about 2 dB in Case XIII and 3 dB in Case XIV. Conversely, after the gap(s), say $x > 75$ m, the extra attenuation becomes systematically less, and before the gap(s), say $x < 45$ m, the extra attenuation is almost unnoticeable. These results suggest that although all patches affect the *SPL* at a receiver because they are diffusely reflective, the patches near the receiver are more effective.

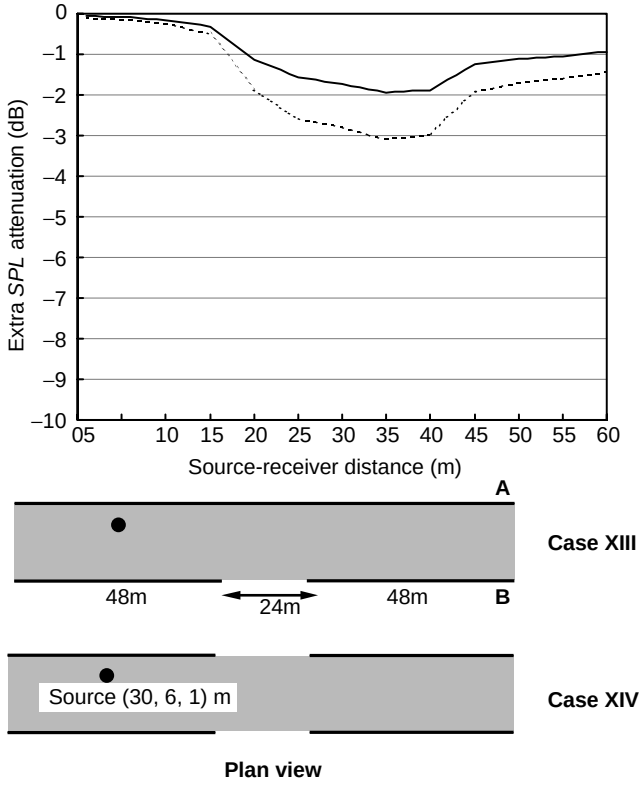

Figure 15. Extra *SPL* attenuation caused by gaps between buildings: (——), Case XIII; (– – –), Case XIV.

3.4. ABSORPTION FROM AIR AND VEGETATION

At relatively high frequencies, air absorption may considerably reduce the sound level in urban streets. The absorption from vegetation may have a similar effect. For the street configuration in section 3.1, the extra *SPL* attenuation caused by air absorption with $M = 0{\cdot}005$, $0{\cdot}015$ and $0{\cdot}025$ Np/m is shown in Figure 16. The three M values correspond approximately to the air absorption at 3, 6 and 8 kHz at a temperature of 20°C and relative humidity of 40–50% [40]. Again, the source is at (30, 6, 1) m and the sound attenuation calculation is based on the average of four receiver lines, namely (31–90, 2, 1) m, (31–90, 2, 18) m, (31–90, 18, 1) m and (31–90, 18, 18) m. From Figure 16, it can be seen that the effect of air absorption is significant. With $M = 0{\cdot}025$ Np/m, for example, the attenuation is 9 dB at a source–receiver distance of 60 m. As expected, due to the increase in average sound path, the extra attenuation increases systematically with increasing source–receiver distance. It is also noted that with diffusely reflecting boundaries the sound path in a street is generally longer than that with geometrically reflecting boundaries and thus, air absorption is more effective [41].

3.5. MULTIPLE SOURCES

The calculations above are based on a single source, which is useful to gain a basic understanding of sound propagation in urban streets. The results are representative of

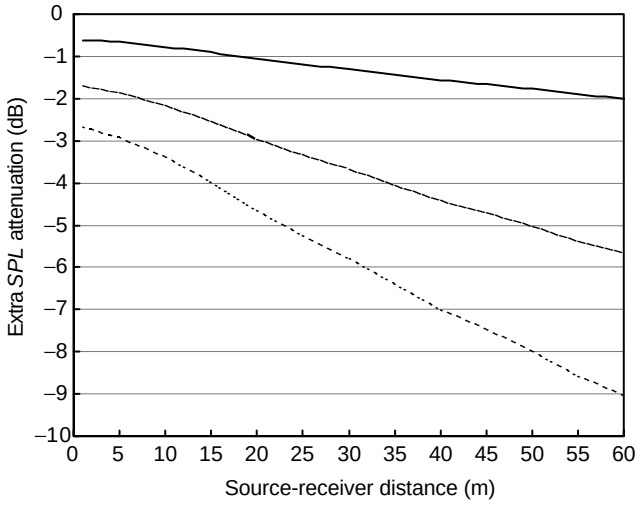

Figure 16. Extra *SPL* attenuation caused by air absorption: ——, $M = 0{\cdot}005$; – – –, $M = 0{\cdot}015$; · · · · · ·, $M = 0{\cdot}025$.

TABLE 1

Extra SPL (dB) attenuation with multiple sources caused by some treatments shown in Figures 11–14 and 16

Cases	$x = 60$ m, $a = 5$ m	$x = 60$ m, $a = 15$ m	$x = 62{\cdot}5$ m, $a = 5$ m	$x = 67{\cdot}5$ m, $a = 15$ m
Figure 11, $\alpha = 0{\cdot}9$	5·6	5·6	5·6	5·6
Figure 12, Case IV	3·3	3·3	3·3	3·3
Figure 13, Case VII	2·3	2·2	2·3	2·2
Figure 14, Case XII	2·5	2·5	2·5	2·6
Figure 16, $M = 0{\cdot}025$	4·1	4·0	4·2	4·3

certain types of urban noise, such as low-density traffic. They are also useful for considering noise propagation from a junction to a street. Certainly, it is also important to consider the situation with multiple sources. If boundary conditions are constant along a street, the sound distribution with multiple sources can be readily calculated by using the data from a single source [42]. Assume that incoherent multiple sources are evenly distributed along the length and the source spacing is a. Table 1 shows the extra *SPL* attenuation with $a = 5$ m and 15 m, caused by some treatments shown in Figures 11–14 and 16. In the calculation, receivers are considered to be in two typical cross-sections: $x = 60$ m, with no horizontal distance from a source; and $x = 62{\cdot}5$ or $67{\cdot}5$ m, halfway between two sources. Corresponding to the calculation with a single source, for each cross-section, an average is made at four receivers, namely (x, 2, 1) m, (x, 2, 18) m, (x, 18, 1) m, and (x, 18, 18) m. By comparing Table 1 with Figures 11–14 and 16, it can be seen that the extra attenuations with multiple sources caused by the treatments highly correlate to the extra attenuations with a single source in the relatively near field. Overall, the results in Table 1 demonstrate that if a treatment is effective with a single source, it is also effective with multiple sources.

4. CONCLUSIONS

A radiosity-based theoretical/computer model, RASCL, has been developed for computing the sound fields in urban streets with diffusely reflecting façades. In the model, the ground can be considered as either diffusely or geometrically reflective. Comparison between the theoretical prediction and the measurement in a scale model of an urban street shows very good agreement. The algorithms have also been validated in other spaces. Note that RASCL is an energy-based model, which ignores wave effects and thus may be inherently inaccurate at lower frequencies.

Using RASCL a series of computations has been carried out for a number of hypothetical rectangular streets. Computation in a typical street shows that though with diffusely reflecting boundaries, the sound attenuation along the length is significant, typically at 20–30 dB/100 m. The sound distribution in a cross-section is generally even unless the cross-section is very close to the source. It has also been demonstrated that if the façades in a street are diffusely reflective, there is no significant difference in the sound field of the street whether the ground is diffusely or geometrically reflective.

The effectiveness of architectural changes and urban design options on increasing sound attenuation along the length in the case of diffusely reflecting boundaries has also been studied using RASCL. The results show that over 2–4 dB extra sound attenuation can be obtained either by increasing boundary absorption evenly or by adding absorption patches on the façades or the ground. Reducing building height has a similar effect. A gap between buildings can provide about 2–3 dB extra sound attenuation, and the effect is more significant in the vicinity of the gap. Air and vegetation absorption is rather effective in increasing sound attenuation along the length, and the extra attenuation could be 3–9 dB at relatively high frequencies. It has also been demonstrated that if a treatment is effective with a single source, it is also effective with multiple sources.

ACKNOWLEDGMENTS

The author is indebted to Raf Orlowski, Paul Richens, David Oldham, Judical Picaut and Peter Tregenza for useful discussions, and to the reviewers of this paper for their valuable comments and suggestions. The financial assistance of the Lloyd's Foundation and the Royal Society is gratefully acknowledged.

REFERENCES

1. F. M. Weiner, C. I. Malme and C. M. Gogos 1965 *Journal of the Acoustical Society of America* **37**, 738–747. Sound propagation in urban areas.
2. R. H. Lyon 1974 *Journal of the Acoustical Society of America* **55**, 493–503. Role of multiple reflections and reverberation in urban noise propagation.
3. H. Kuttruff 1975 *Acustica* **32**, 57–69. Zur Berechnung von Pegelmittelwerten und Schwankungsgrößen bei Straßenlärm.
4. R. Bullen and F. Fricke 1976 *Journal of Sound and Vibration* **46**, 33–42. Sound propagation in a street.
5. H. G. Davies 1978 *Journal of the Acoustical Society of America* **64**, 517–521. Multiple-reflection diffuse-scattering model for noise propagation in streets.
6. M. V. Sergeev 1979 *Soviet Physics—Acoustics* **25**, 248–252. Scattered sound and reverberation on city streets and in tunnels.
7. D. J. Oldham and M. M. Radwan 1994 *Building Acoustics* **1**, 65–87. Sound propagation in city streets.

8. S. Wu and E. Kittinger 1995 *Acustica/Acta Acustica* **81**, 36–42. On the relevance of sound scattering to the prediction of traffic noise in urban streets.
9. K. Heutschi 1995 *Acustica/Acta Acustica* **81**, 26–35. Computermodell zur Berechnung von Bebauungszuschlägen bei Straßenverkehrslärm.
10. D. C. Hothersall, K. V. Horoshenkov and S. E. Mercy 1996 *Journal of Sound and Vibration* **198**, 507–515. Numerical modelling of the sound field near a tall building with balconies near a road.
11. J. Picaut, L. Simon and J. Hardy 1999 *Journal of the Acoustical Society of America* **106**, 2638–2645. Sound field modeling in streets with a diffusion equation.
12. K. K. Iu and K. M. Li 2000 *Proceedings of the Seventh Western Pacific Regional Acoustics Conference, Kumamoto, Japan*, 811–814. The propagation of sound in city streets.
13. J. Kang 2000 *Journal of the Acoustical Society of America* **107**, 1394–1404. Sound propagation in street canyons: comparison between diffusely and geometrically reflecting boundaries.
14. J. Picaut and L. Simon 2001 *Applied Acoustics* **62**, 327–340. A scale model experiment for the study of sound propagation in urban areas.
15. R. Siegel and J. Howell 1981 *Thermal Radiation Heat Transfer.* Washington, DC: Hemisphere, second edition.
16. F. X. Sillion and C. Puech 1994 *Radiosity and Global Illumination.* San Francisco: Morgan Kaufmann Publishers, Inc.
17. G. R. Moore 1984 *Ph.D. Dissertation, University of Cambridge*. An Approach to the Analysis of Sound in Auditoria.
18. T. Lewers 1993 *Applied Acoustics* **38**, 161–178. A combined beam tracing and radiant exchange computer model of room acoustics.
19. J. Kang 2002 *Acustica/Acta Acustica* **88**, 77–87. Reverberation in rectangular long enclosures with diffusely reflecting boundaries.
20. R. Stibbs 1971 *Working Paper No.* 54*, The Martin Centre, University of Cambridge*. The prediction of surface luminances in architectural space.
21. J. D. Foley, A. van Dam, S. K. Feiner and J. F. Hughes 1990 *Computer Graphics: Principle and Practice*. Reading, MA: Addison-Wesley, second edition.
22. M. F. Cohen and D. P. Greenberg 1985 *Computer Graphics* **19**, 31–40. The hemi-cube: a radiosity solution for complex environments.
23. P. Steenackers, H. Myncke and A. Cops 1978 *Acustica* **40**, 115–119. Reverberation in town streets.
24. N. W. M. Ko and C. P. Tang 1978 *Journal of Sound and Vibration* **56**, 459–461. Reverberation time in a high-rise city.
25. J. Kang 1995 *Building Acoustics* **2**, 391–402. Experimental approach to the effect of diffusers on the sound attenuation in long enclosures.
26. J. Kang and R. Neubauer 2001 *Proceedings of the 17th International Congress on Acoustics, Rome*, 7A.10.02. Predicting reverberation time: comparison between analytic formulae and computer simulation.
27. H. Kuttruff 1997 *Acustica/Acta Acustica* **83**, 622–628. Energetic sound propagation in rooms.
28. M. Hodgson 1991 *Journal of the Acoustical Society of America* **89**, 765–771. Evidence of diffuse surface reflections in rooms.
29. S. N. Chandler-Wilde and D. C. Hothersall 1995 *Journal of Sound and Vibration* **180**, 705–724. Efficient calculation of the green function for acoustic propagation above a homogeneous impedance plane.
30. K. Attenborough and T. Waters-Fuller 2000 *Journal of the Acoustical Society of America* **108**, 949–956. Effective impedance of rough porous ground surfaces.
31. K. M. Li, S. Taherzadeh and K. Attenborough 1998 *Journal of the Acoustical Society of America* **104**, 2077–2083. An improved ray-tracing algrithm for predicting sound propagation outdoors.
32. M. C. Bérengier, M. R. Stinson, G. A. Daigle and J. F. Hamet 1997 *Journal of the Acoustical Society of America* **101**, 155–162. Porous road pavements: acoustical characterization and propagation effects.
33. K. K. Iu and K. M. Li 2001 *Proceedings of the Eighth International Congress on Sound and Vibration, Hong Kong*, 1309–1314. The propagation of sound in long enclosures with geometrically reflecting boundaries.
34. Edinburgh University Data Library *http://digimap.edina.ac.uk/* Edinburgh Data and Information Access EDINA Digimap.

35. J. KANG, J. Y. TSOU and S. LAM 2001 *Proceedings of the Eighth International Congress on Sound and Vibration, Hong Kong*, 1241–1248. Sound propagation in urban streets: comparison between UK and Hong Kong.
36. B. KOTZEN and C. ENGLISH 1999 *Environmental Noise Barriers: A Guide to Their Acoustic and Visual Design*. London: Spon Press.
37. K. V. HOROSHENKOV and M. J. SWIFT 2001 *Applied Acoustics* **62**, 665–690. The effect of consolidation on the acoustic properties of loose rubber granulates.
38. J. KANG 2000 *Proceedings of the Institute of Acoustics (IOA) (U.K.), Liverpool*, **22**, 163–170. Sound field in urban streets with diffusely reflecting boundaries.
39. J. KANG 2001 *Environment and Planning B: Planning and Design* **28**, 281–294. Sound propagation in interconnected urban streets: a parametric study.
40. American National Standard ANSI S1.26 1978 *Method for the Calculation of the Absorption of Sound by the Atmosphere*.
41. J. KANG 2002 *Acoustics of Long Spaces: Theory and Design Practice*. London: Thomas Telford.
42. J. KANG 1996 *Journal of the Acoustical Society of America* **99**, 985–989. Acoustics in long enclosures with multiple sources.